Effect of a Gradient Static Magnetic Field on an Unstirred Belousov−Zhabotinsky Reaction by Changing the Thickness of the Medium

Hideyuki Okano,*,† Hiroyuki Kitahata,‡,§ and Daisuke Akai‖

International Innovation Center, Kyoto University, Yoshida-Honmachi, Sakyo-ku, Kyoto 606-8501, Japan, Department of Physics, Graduate School of Science, Kyoto University, Kitashirakawa-Oiwake-cho, Sakyo-ku, Kyoto 606-8502, Japan, and Bioengineering Laboratory, Graduate School of Engineering, Kyoto University, Yoshida-Honmachi, Sakyo-ku, Kyoto 606-8501, Japan

Received: May 23, 2008; Revised Manuscript Received: November 25, 2008

The anomalous chemical wave propagation of an unstirred Belousov−Zhabotinsky (BZ) reaction was observed under exposure to a gradient static magnetic field (SMF). The gradient SMF effect on the BZ reaction was investigated by increasing the thickness of the BZ medium up to 0.9 mm under the conditions of the extremely reduced water evaporation and surface tension caused by air−water interfaces. The respective maximum values of magnetic flux density (B_{max}), magnetic flux gradient (G_{max}), and the magnetic force product of the magnetic flux density × its gradient (a magnetic force parameter) are 0.206 T, 37 T m^{-1}, and 4 T^2 m^{-1}. The experiments demonstrate that the more increased thickness of the BZ medium induces the larger anomalous wave propagation toward the peak magnetic gradient line but not toward the peak magnetic force product line. The anomalies were significantly enhanced by the increased thickness of the BZ medium at the shorter distance from the maximum magnetic gradient point. The possible mechanism of SMF-induced anomalous wave propagation related to the BZ medium thickness is that the micro-magneto-convection-induced flow of the paramagnetic iron ion complexes at the wavefronts can be accelerated by increases in both the spatial magnetic gradient and the volumetric depth of the diffusion layer.

Introduction

The Belousov−Zhabotinsky (BZ) reaction, i.e., the catalyzed oxidation of malonic acid in the presence of bromide, bromate, and an inorganic catalyst, is more frequently studied as a simplified experimental model of a nonequilibrium open system.[1] Various studies have been performed concerning the modifiers on the BZ reaction, such as electromagnetic fields, electric fields, illumination, gravity, viscosity, and so forth. However, there has not been a report on the effects of static magnetic fields (SMF) on a stirred BZ reaction.[2] In contrast, recently, we found that the wave velocity of an unstirred BZ reaction at the depth of 1.3 mm was accelerated primarily by a magnetic gradient of static magnetic fields (SMF), and thereby the anomalous chemical wave propagation was induced particularly along the peak magnetic gradient line.[3] It is suggested that the interaction mechanism between the concentration gradient and the magnetic gradient plays a major role in the anomalous wave propagation through increased concentration gradient of the paramagnetic iron ion complexes at the wavefronts.[3]

The local magnetic force F_x per unit volume acting on the BZ solution along the x-axis is given according to the following equation[4]

$$F_x = c\chi\left(B_x\frac{\partial B_x}{\partial x} + B_y\frac{\partial B_x}{\partial y} + B_z\frac{\partial B_x}{\partial z}\right) \approx cB_xG_x \qquad (1)$$

where c = molar concentration; χ = molar magnetic susceptibility; $\mathbf{B} = (B_x, 0, 0)$, local magnetic flux density; $\mathbf{G} = (G_x, 0, 0)$, local magnetic gradient; xyz is the coordinate system in real space. The maximum force product value of B_x (0.15 T) × G_x (20 T m^{-1}) along the x-axis is calculated to be 3 T^2 m^{-1} at a specific point between magnets, whereas this peak point is not equal to the peak points of maximum intensity (B_{max}) or maximum gradient (G_{max}) due to the complex magnetic field configuration applied in this experiment. The χ values of Fe(II) and Fe(III) complexes are in the range of (8.0−15.0) × 10^{-3} cm^3 mol^{-1} at room temperature,[5] and the estimated molar concentrations of Fe(II) and Fe(III) complexes are 4 mM. Therefore, the estimated values of F_x are in the range of 0.096−0.180 mN cm^{-3} using eq 1. However, the most anomalous wave propagation was observed along the peak magnetic gradient line, but not along the peak force product line.[3] The factors involved in the reaction-diffusion systems under SMF exposure are that the concentration gradient of the paramagnetic iron ion complexes at the wavefronts could be associated with the spatial magnetic gradient rather than the magnetic force.[3] Thus, in our previous study,[3] the SMF effects on the wave propagation were analyzed as a quasi-two-dimensional system for simplicity. However, lines of magnetic force in the experimental setup are obviously not two dimensional but three dimensional. The SMF effects on the reduced thickness less than 1 mm of the BZ medium have not been investigated, even though it is reported that the paramagnetic medium thickness of 1 mm is thick enough for solution convection under gradient SMF exposure.[6]

* To whom correspondence should be addressed. Phone: +75-753-9201. Fax: +75-753-9201. E-mail: okano@iic.kyoto-u.ac.jp.
† International Innovation Center, Kyoto University.
‡ Department of Physics, Graduate School of Science, Kyoto University.
§ Current address: Department of Physics, Graduate School of Science, Chiba University, Chiba 263-8522, Japan.
‖ Bioengineering Laboratory, Graduate School of Engineering, Kyoto University.

10.1021/jp8045565 CCC: $40.75
Published on Web 03/09/2009

Focusing on the geometrical analysis of the interaction between the magnetic field distribution and the chemical wave propagation, the present study was undertaken to examine the gradient SMF effect on the BZ reaction by changing the thickness of the BZ medium. The unstirred BZ system was applied to investigate the relationship mechanism between the thickness of the BZ solution and the magnetic gradient. To avoid or eliminate the water evaporation (water vaporization) and surface tension caused by air−water interfaces, the BZ solution was infused between the two acrylic plates with the gap-depth placed on the magnet. The thickness of the BZ medium was changed between the gap depth of two acrylic plates using glass plate spacers.

Experimental Section

The preparation of the BZ solution was the same as previously reported.[3] Briefly, two chemicals, 1,10-phenanthroline monohydrate and iron(II) sulfate heptahydrate, were purchased from Sigma-Aldrich Chemical. All other chemicals were obtained from Wako Pure Chemical and Kishida Chemical. All chemicals were analytical grade reagents and used without further purification. A 20 mL portion of the BZ solution was used per experiment. An aqueous solution of ferroin, tris(1,10-phenanthroline)iron(II) sulfate, was prepared by hand-mixing the stoichiometric amounts of 1,10-phenanthroline monohydrate ($C_{12}H_8N_2 \cdot H_2O$) and iron(II) sulfate heptahydrate ($FeSO_4 \cdot 7H_2O$) in pure water. The water was purified using a Millipore Milli-Q system. The BZ medium in the excitable state contains water, 0.15 M sodium bromate ($NaBrO_3$), 0.30 M sulfuric acid (H_2SO_4), 0.10 M malonic acid ($CH_2(COOH)_2$), 0.03 M sodium bromide (NaBr), and 4.0 mM ferroin ($[Fe(phen)_3]^{2+}$).

The SMF was generated a magnetic device as described elsewhere.[3] Briefly, the magnetic device is constructed of a pair of rectangular neodymium magnets (NdFeB, B_{max} 0.5 T, 80 [length] × 17 [width] × 52 [height] mm, TDK) (Figure 1). The opposite polarity magnets attracting each other through a 26 mm air gap are fixed parallel to both sides of the stainless frame. The rectangular zone between the internal edges of the magnets is 26 × 80 mm (Figure 1). Since it is reported that the magnetic poles (N or S) have no significant influence on the shape of the waves at any point and the results appear symmetrical as to the center line (the *y*-axis) of the two magnets,[3] in this study the measurements and analyses of the magnetic field distribution and chemical wave propagation of semicircular waves were carried out in the right side of the magnetic device. Two parallel transparent acrylic plates (100 [length] × 100 [width] × 2 [height] mm, 7558AL 100 × 100 × 2C, Tokyu Hands) were placed on the right side magnet indicating N-polarity at the internal edge and S-polarity at the external edge (Figure 1).

The magnetic field distributions were measured and analyzed in the three-dimensional *x*−*y*−*z* plane up to 70 mm from the trigger point at 3 mm over the magnetic device using a gaussmeter (model 4048, Hall probe A-4048−002, Bell Technologies) and a LabVIEW image analysis software (National Instruments). This 3 mm distance was fixed by imposing space between the magnet and the wall of the lower plate (2 mm thickness) using a 1 mm thickness spacer. For the fixed distance of 3 mm between the reactor and the magnet, the position of the vertical *z*-axis is $z = 0$.

The respective maximum values of magnetic flux density (B_{max}), magnetic flux gradient (G_{max}), and the magnetic force product of the magnetic flux density × its gradient (a magnetic force parameter) are 206 mT (0.206 T) ($x = 0$ mm, $y = 0$ mm, $z = 0$ mm), 37 mT mm^{-1} (37 T m^{-1}) ($x = 13$ mm, $y = 0$ mm, $z = 0$ mm), and 4000 mT^2 mm^{-1} (4 T^2 m^{-1}) ($x = 0$ mm, $y = 0$ mm, $z = 0$ mm) (Figure 2). The B_{max} of ∼206 mT is measured at the trigger point in the center of the magnetic device and the G_{max} of 37 mT mm^{-1} is obtained at the internal edge of the magnet along the center line (the *x*-axis) (Figure 2). For the vertical *z*-direction, the maximum value of magnetic force parameter $|\mathbf{B} \times \mathbf{G}|_{max}$ is estimated to be 4 T^2 m^{-1} at the $z = 0$ mm (Figure 2C). While the medium thickness is increased up to 0.9 mm along the *z*-axis, the parameters for SMF exposure are in the narrow range of $B_z = 0.190-0.206$ T, $G_z = 16.8-19.4$ T m^{-1}, and $|\mathbf{B} \times \mathbf{G}| = 3.2-4.0$ T^2 m^{-1} for addressing the $z = 0-0.9$ mm (Figure 2C).

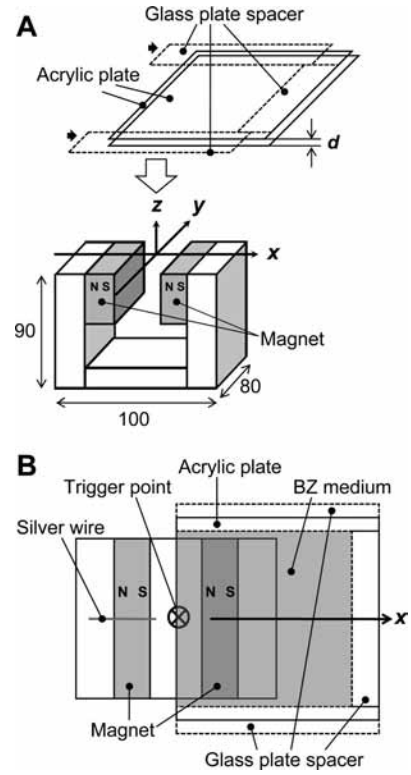

Figure 1. An experimental setup (units in millimeters). (A) The BZ medium was infused between the two acrylic plates with the gap-depth (*d*) placed on the right side magnet indicating three field directions (*x*, *y*, *z*). (B) Shortly thereafter, the initiation of the BZ reaction was performed at the trigger point (a cross circle) of the lower acrylic plate in the center of the magnetic device using a silver wire.

The measured intensity in the sham exposed plates using a geomagnetometer (IDR-321, Integrity Design & Research) is ∼50 μT, which is almost the same as the background geomagnetic field intensity in our laboratory (∼46−47 μT, data from WDC for Geomagnetism). Except for the geomagnetic field, the sham exposed plates were not exposed to any magnetic field. The sham experiment was performed using a sham exposure unit with sham magnets of steel materials to compare the effects. The sham exposure unit was apparently the same configuration with SMF exposure unit except for the materials of the magnets. No measurable temperature change (±0.03 °C) in the BZ medium was observed in any magnetic flux density and gradient point of SMF exposure unit and in any point of the sham exposure unit using a thermosensor (model DS-RTD, sensor PT-100, MK Scientific) (data not shown). Therefore, there was no detectable heat exchange or transfer in both cases between the magnets (or the sham magnets) and the BZ solution. This also indicates that the SMF itself did not change the endothermic and exothermic processes of the BZ reaction, while it is reported

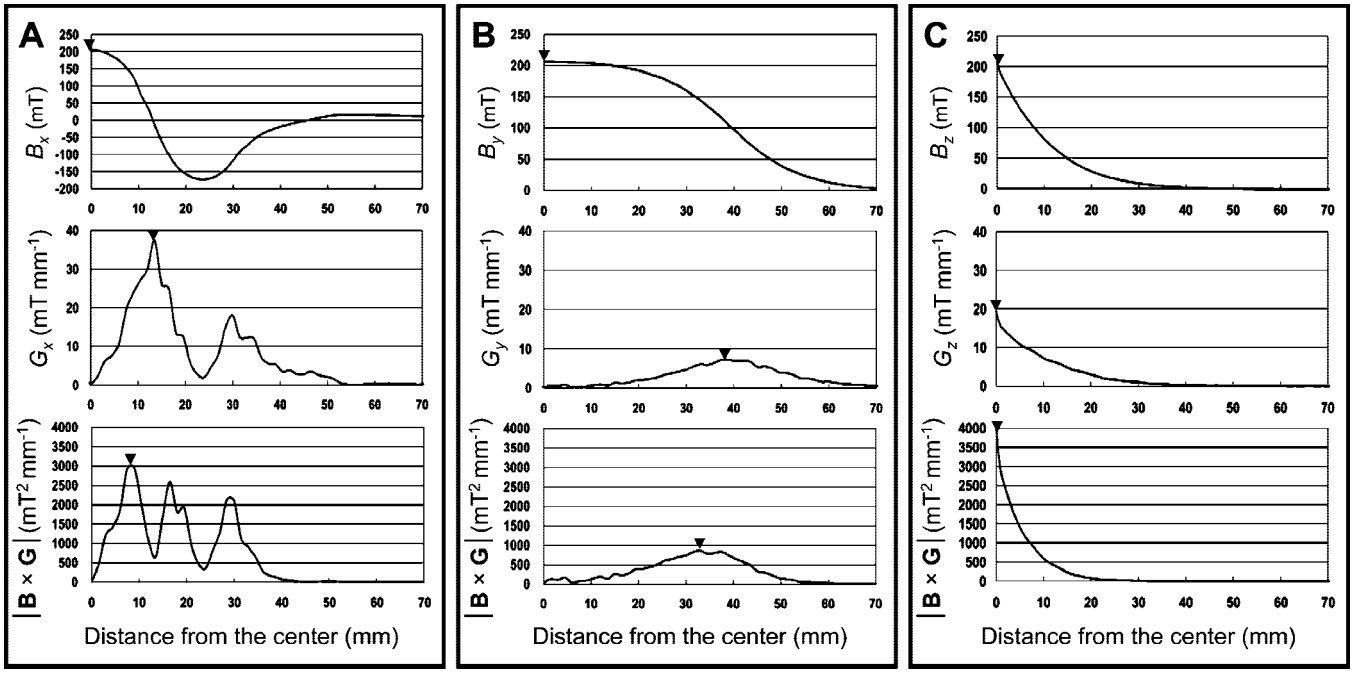

Figure 2. (A) Magnetic distribution of the *x*-axis. (B) Magnetic distribution of the *y*-axis. (C) Magnetic distribution of the *z*-axis. Upper, the magnetic flux density values; middle, the magnetic flux gradient values; lower, the magnetic force product values. (▼) The respective peak value.

that with increase in ambient temperature, the wave propagation velocities are accelerated.[7]

Eight experimental groups with and without SMF exposure were examined with changing the thickness of the BZ medium: 0.3, 0.5, 0.7, and 0.9 mm. The thickness of the BZ medium (the gap-depth of two acrylic plates) was changed using spacers consisting of a variable number of glass plates (e.g., 0.1 mm thickness) stacked on each other (Figure 1). The volume of the BZ medium in each experimental group increased with the increasing depth. Within 3 min after mixing the components of the BZ medium, the BZ solution was infused between the two acrylic plates with the gap-depth placed on the magnet (the timing of applying the SMF) or sham magnet using a pipet (Pipetman P-1000, Gilson). The sham and SMF experiments were performed under the same condition. Almost immediately after the SMF was applied, the chemical waves were triggered in the unstirred BZ solution (the delay interval of SMF application and chemical wave generation was within 10 s). The measurements were started ($t = 0$) just after triggering the chemical waves. The chemical waves were initiated at the trigger point of the lower acrylic plate in the center of the magnetic device using a silver wire. In the SMF experimental group, the BZ medium was exposed to SMF for a period of up to 8 min at 298 K. The images were captured with a resolution of 640 × 480 pixels (VGA) at a frame rate of 30 frames per second (fps) by a digital video camera (NV-GS250, Panasonic) from above. The images of the target pattern in chemical waves were quatified using Image J (NIH image) and Scion Image (ver. 4.0.3.2) software package. All the experiments were carried out at 298 K.

Differences in mean values between each SMF experimental group and the corresponding sham experiment group were analyzed by the Mann−Whitney *U*-test for pairwise comparisons between groups. All values are expressed as mean ± standard deviation. Differences between experiments were considered statistically significant at probability (*P*) values of <0.05.

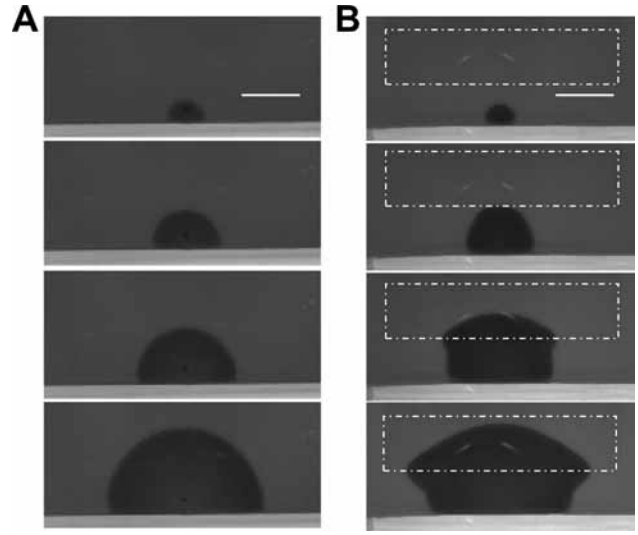

Figure 3. Temporal changes in the images of a single wave propagation at the depth of 0.9 mm (2, 4, 6, and 8 min after the initiation of the BZ reaction at 298 K; scale bar = 20 mm). (A) A sham experiment. (B) A SMF experiment (the outline of a magnet is shown in the dashed-dotted line).

Results

A single and multiple semicircular wave patterns were propagated in the sham experiment. The simplest example is a single semicircular wave with the first wavefront (Figure 3A). In any case, the whole color of the intact solution was red at the beginning. After the central edge of the lower plate was triggered, blue semicircular waves spread from the trigger point. Finally, the waves vanished at the edge of the plate spacers with limited space (figure not shown).

In contrast to the sham experiment, SMF exposure induced an anomalous wave propagation with a single wave or multiple waves particularly along the internal edge of the magnet. The simplest example is a single semicircular wave with the first

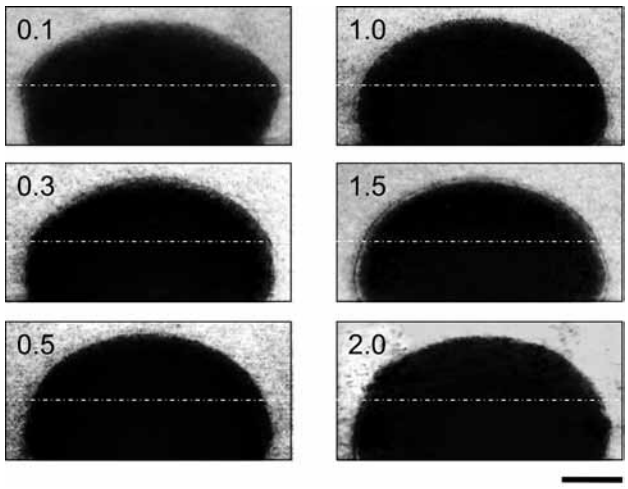

Figure 4. The images of a single wave propagation at variable distances from the $z = 0$ plane at a fixed medium thickness of $d = 0.9$ mm (units, mm; scale bar = 10 mm). The images were obtained 8 min after the initiation of the BZ reaction at 298 K under SMF exposure (an internal edge of a magnet is shown in dashed-dotted line).

wavefront, and the anomalies of wave propagation were strongest along the internal edge of the magnet (Figure 3B). About 8 min after the initiation of the BZ reaction, the wavefront reached the external edge of the magnet. The observation was terminated at this point. Thereafter, the wave propagation was suppressed due to the configuration of magnet, and finally the waves faded out at the edge of the plate spacers or were collided and fused by another wave spontaneously initiated at the edge of the plate spacers (figure not shown).

As shown in Figure 3A, to estimate the roundness of wavefronts without SMF exposure or, alternatively, as shown in Figure 3B, to evaluate the extent of anomaly (noncircularity) of wave propagation induced by the SMF, the radian measure of the angle was carried out as a circularity parameter of wave propagation. To simplify the analysis of the pattern dynamics and minimize its variance, only a single semicircular wave propagation was analyzed.

As preliminary studies on the distance effect of SMF on the BZ reaction by changing the space distance along the vertical z-axis between the reactor and the magnet, the anomalies of wave propagation at a fixed medium thickness of $d = 0.9$ mm were diminished with the distance from the $z = 0$ plane and apparently disappeared at the distance of approximately 2.0 mm (Figure 4).

The angle (θ) was measured by the internal edge of the magnet (the peak magnetic gradient line) and the tangential line of the wavefront along the internal edge of the magnet (Figure 5A). About 4 min after the initiation of the BZ reaction, the wavefront reached the internal edge of the magnet (Figure 5B). The 0 rad (the minimum value) position of the wavefront is shown as the null angle formed at the cross point of the internal edge of the magnet and the center line (the x-axis). The cross point is coincident with the highest magnetic gradient point. As the wavefront spreads along the internal edge of the magnet, the anomalies of wave propagation become stronger and the angle becomes closer to $\pi/2$ rad (the maximum value) (Figure 5C).

Changes in the radian measure of the angle (θ) values of wave propagation were plotted against the distance (a) from the cross point by changing the depth (d) of the BZ medium (Figure 6A). SMF exposure induced significant increases in the θ values throughout the a values ranging 5−35 mm at the d

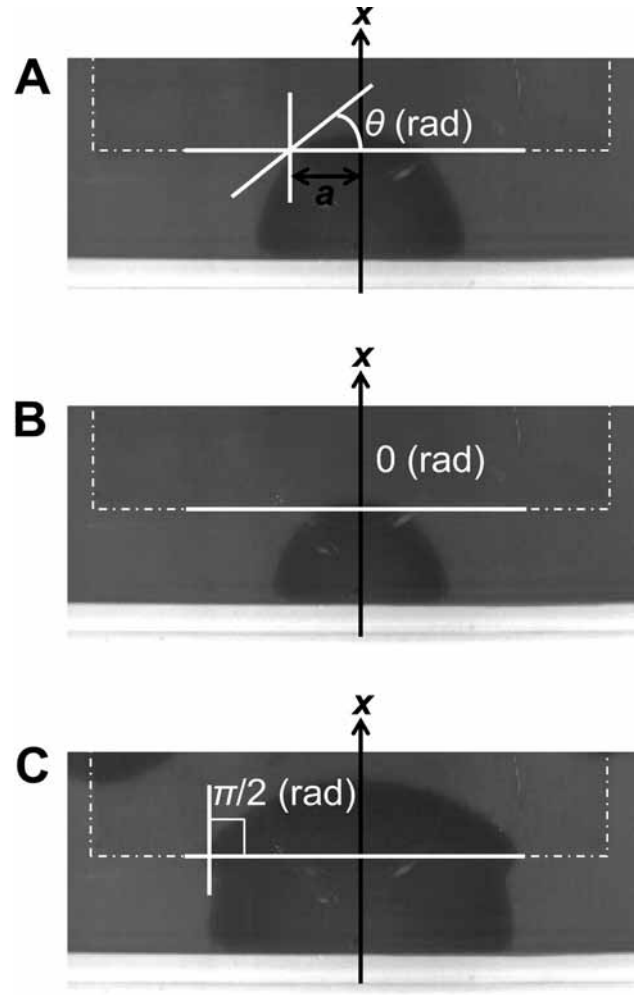

Figure 5. The radian measure of the angle of wave propagation. (A) The angle (θ) was formed by the internal edge of the magnet (the peak magnetic gradient line) and the tangential line of the first wavefront along the internal edge of the magnet or sham magnet. a, the distance from the cross point formed by the internal edge of the magnet and the x-axis. (B) The angle in this case is 0 rad. (the outline of a magnet is shown in the dashed-dotted line). (C) The angle in this case is $\pi/2$ rad (the outline of a magnet is shown in the dashed-dotted line).

values of 0.3−0.9 mm, compared with the sham experiment (Figure 6A). The larger d values correspond to the larger initial increases in the θ values in the smaller a values (the shorter distance), and for the thicker layer, the θ values increase more rapidly to reach the maximum angle ($\pi/2$).

In the sham experiment, the following approximation and simulation for the concentric circles (roundness) of the chemical wave propagation can be applied to the measured θ values

$$\theta = \arctan(a/a_0) \tag{2}$$

where a = the distance from the cross point; $a_0 = 13$ mm which is the length between the internal edge of the sham magnet and the trigger point (the center of circles). In the SMF experiment, however, eq 2 is not applicable to the measured θ values. Establishing a theoretical model for SMF experiment remains a future work.

The largest differences of the θ values between both experiments were observed at $a = 20$ mm in $d = 0.3$ mm (the SMF/sham ratio = 1.10), at $a = 20$ mm in $d = 0.5$ mm (the ratio =

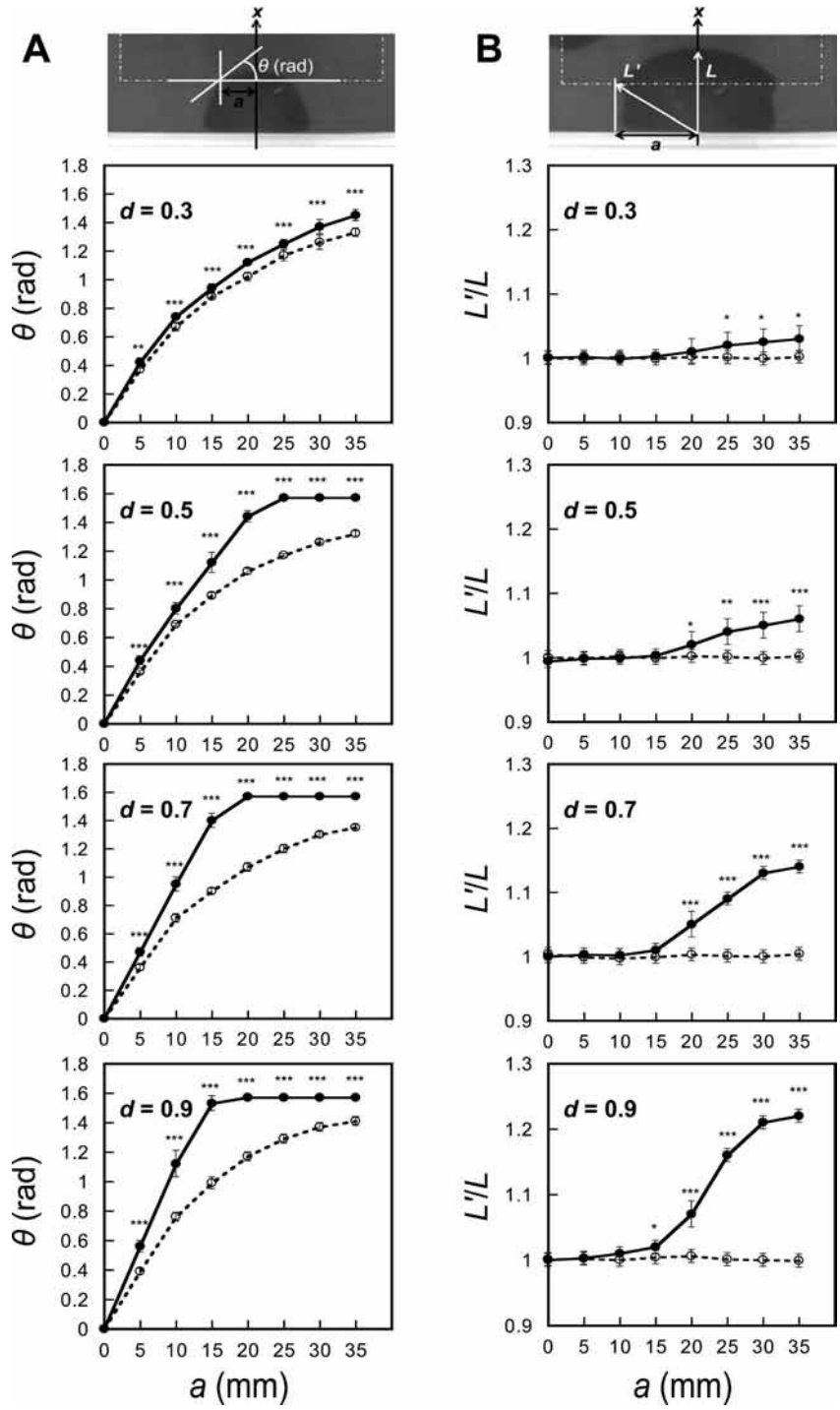

Figure 6. Changes in (A) the angle (θ) or (B) the extent of anomaly (L'/L) of wave propagation in sham (○) and SMF (●) experiments by changing the depth (d) of the BZ medium. θ, the angle formed by the internal edge of the magnet (or sham magnet) and the tangential line of the first wavefront along the internal edge of the magnet (or sham magnet); L'/L, the ratio of the L' distance to the L distance for each direction of the propagation from the trigger point; a, the distance from the cross point. $n = 8$ for each group. $^*P < 0.05$, $^{**}P < 0.01$, $^{***}P < 0.001$ from the corresponding sham experiment.

1.36), at $a = 15$ mm in $d = 0.7$ mm (the ratio = 1.56), and at $a = 15$ mm in $d = 0.9$ mm (the ratio = 1.55).

Changes in the extent of anomaly (L'/L) of wave propagation were also plotted against the a values by changing the d values of the BZ medium (Figure 6B). The larger L'/L values directly correlated with the larger noncircularity of wave propagation. SMF exposure induced significant increases in the L'/L values at $a = 25-35$ mm in $d = 0.3$ mm, at $a = 20-35$ mm in $d = 0.5$ mm, at $a = 20-35$ mm in $d = 0.7$ mm, and at $a = 15-35$ mm in $d = 0.9$ mm, compared with the sham experiment (Figure 6B). The larger d values correspond to the increasing L'/L values at least in the range of $a = 20-35$ mm, and the a values are positively correlated with the L'/L values. The largest differences of the L'/L values between both experiments were observed at $a = 35$ mm in all of the depths investigated (the SMF/sham ratio: 1.03 in $d = 0.3$ mm, 1.06 in $d = 0.5$ mm, 1.14 in $d = 0.7$ mm, and 1.22 in $d = 0.9$ mm).

Temporal changes in the θ values or L'/L values between both experiments were also analyzed by changing the d values (Figure 7). Figure 7A shows the experimental observation of

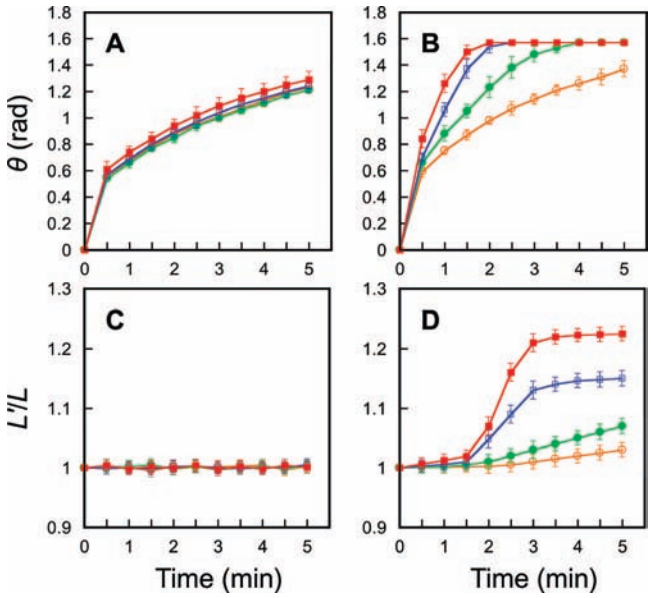

Figure 7. Temporal changes in the angle (θ) or the extent of anomaly (L'/L) of wave propagation in the sham and SMF experiments by changing the depth (d) of the BZ medium. (A) θ in the sham, (B) θ in the SMF, (C) L'/L in the sham, (D) L'/L in the SMF experiments. $n = 8$ for each group. (open orange circles) $d = 0.3$ mm, (solid green circles) $d = 0.5$ mm, (open blue boxes) $d = 0.7$ mm, and (solid red boxes) $d = 0.9$ mm.

the radian measure of the angle as a function of time (t) in the sham experiment; the θ values of wave propagation increased gradually and similarly regardless of the increasing d values ranging 0.3−0.9 mm. In this figure, $t = 0$ indicates the time at which $a = 0$ mm (the first wavefront reached the internal edge of the magnet or sham magnet). In contrast, in the SMF experiment, the θ values of wave propagation increased more rapidly and differently with the increasing d values ranging 0.3−0.9 mm (Figure 7B).

In the sham experiment, the L'/L values of wave propagation stayed constant because of the roundness of the wave propagation in the range of d values analyzed (Figure 7C). In contrast, in the SMF experiment, the L'/L values of wave propagation increased more rapidly and differently with the increasing d values ranging 0.3−0.9 mm (Figure 7D).

Discussion

Both θ and L'/L values are used to evaluate the roundness of the chemical wave propagation. The θ measurement appears a more sensitive and early indicator of anomalies of wave propagation than the method of measuring L'/L. The results indicate that SMF exposure significantly enhanced the anomalies of wave propagation particularly along the peak magnetic gradient line, but not along the peak force product line, compared with the sham exposure. The larger depth induced the larger increases in the anomalies of wave propagation at the shorter distance from the maximum magnetic gradient point. It has been proposed that the interaction of magnetic flux density and concentration gradient depending on the magnetic susceptibility of metal ions,[8] and the micro-magneto-convection effect inside the diffusion layer of the metal ions.[9] In this respect, our present study suggests that the micro-magneto-convection-induced flow of the paramagnetic iron ion complexes at the wavefronts can be accelerated by both increases in the spatial magnetic gradient and the volumetric depth of the diffusion layer.

For the distance effect of SMF on the BZ reaction by changing the space distance along the vertical z-axis between the reactor and the magnet, the anomalies of wave propagation at a fixed medium thickness of $d = 0.9$ mm were diminished with the distance from the $z = 0$ plane and apparently disappeared at the distance of approximately 2.0 mm (Figure 4). Three magnetic parameters decay exponentially with the distance from the $z = 0$ plane, and the precise boundaries between the anomalous and normal states are not determined but are estimated to be close to the $z = 2.0$ mm distance, where the parameters for SMF exposure are approximately $B_z = 0.168$ T, $G_z = 14$ T m^{-1}, and $|\mathbf{B} \times \mathbf{G}| = 2.35$ T^2 m^{-1} for addressing the $z = 2.0$ mm (Figure 2). When the thickness of the BZ medium is analyzed, however, the threshold exposure condition of SMF on the shape of wave propagation in more reduced thickness ($d < 0.3$ mm) has not been investigated in detail. Therefore, further study will be necessary to delineate the underlying mechanism and threshold exposure condition of SMF on the BZ reaction.

In the effects of SMF on water evaporation and water surface tension, it was reported that strong magnetic-gradient-induced forces promote water evaporation (8 T, 400 T^2 m^{-1}),[10] and change water surface tension (15 T, 1500 T^2 m^{-1}).[11] In this study, however, the gradient SMF effect on water evaporation and surface tension could be negligible since the magnetic-gradient-induced force (0.206 T, 4 T^2 m^{-1}) is too small to induce a detectable change in these phenomena. Instead, the gradient SMF effect on the BZ reaction was investigated under the conditions of the extremely reduced evaporation and surface tension using two plates, and thereby the decrease in the gap-depth of two plates may increase water retention, irrespective of with and without SMF exposure.

The magnetic-gradient-induced force effects (8 T, 410 T^2 m^{-1}) have been reported on the separation or movement of transition-metal ions, including iron ions.[12] According to other studies concerning the SMF effects on chemical wave propagation, the effects of a gradient SMF (up to 1.4 T) on wavefront propagation have been demonstrated using a nonphysiological, unstirred, O_2-saturated glacial acetic acid solution containing 0.98 M benzaldehyde and 7.5 mM Co(II) acetate.[13] The magnetic field strength and gradient used in these experiments were not given explicitly, but the maximum force product ($|\mathbf{B} \times \mathbf{G}|$) values were estimated to be approximately in the range of 5−10 T^2/m.[14] These results suggest the ability of magnetic forces explained by invoking a combination of diamagnetic and paramagnetic forces to determine the position of the wavefront.[13] It is shown that paramagnetic $Co^{II}EDTA^{2-}$ and diamagnetic $Co^{III}EDTA^{-}$ cannot be separated from homogeneous solution, and it is therefore concluded that heterogeneities of both the solution and the characteristics of the applied SMF are essential for the evolution of the effects.[13a] Although paramagnetic ferroin (Fe^{II} complex) and ferriin (Fe^{III} complex) in the BZ solution have not been separated using the magnetic gradient or force, the previous study suggested that the movement or concentration change of ferroin under SMF exposure could play a dominant role in the anomalous wave propagation in the BZ reaction.[3] It is therefore concluded that heterogeneities of both the increased amount of at least one iron ion complex in the thicker diffusion layer and the applied SMF configuration play a pivotal role in the enhancement of the anomalous wave propagation.

Acknowledgment. We are very grateful to Dr. Kouji Takano (Takano Original Magnet Inc., Tsukuba, Japan) for measurement and analysis of spatial distribution of magnetic flux density in the magnet.

References and Notes

(1) Zaikin, A. N.; Zhabotinsky, A. M. *Nature* **1970**, *225*, 535. Scott, S. K.; Showalter, K. *Chemical Waves and Patterns*; Kapral, R., Showalter, K., Eds.; Kluwer Academic Publishers: Dordrecht, 1995; p 485.

(2) Blank, M.; Soo, L *J. Cell. Biochem.* **2001**, *81*, 278. Blank, M., Soo. L. Bioelectrochemistry 2003. *61* 93. Sontag, W *Bioelectromagnetics* **2006**, *27*, 314.

(3) Okano, H.; Kitahata, H.; Akai, D.; Tomita, N. *Bioelectromagnetics* **2008**, *29*, 598.

(4) Evans, R.; Timmel, C. R.; Hore, P. J.; Britton, M. M. *J. Am. Chem. Soc.* **2006**, *128*, 7309.

(5) Lide, D. R. *CRC Handbook of Chemistry and Physics (88th Edition 2007−2008*) Lide. R. D., Ed.; CRC Press: Boca Raton, FL, 2007; pp 4−142.

(6) Katsuki, A.; Tanimoto, Y. *Chem. Lett.* **2005**, *34*, 726.

(7) Zhang, J.; Zhou, L.; Ouyang, Q *J. Phys. Chem. A.* **2007**, *111*, 1052.

(8) Duan, W.; Kitamura, S.; Uechi, I.; Katsuki, A.; Tanimoto, Y. *J. Phys. Chem. B* **2005**, *109*, 13445. Tanimoto. Y. *Magneto-Science; Magnetic Field Effects on Materials: Fundamentals and Applications*; Yamaguchi, M. ; Tanimoto. Y., Eds.;Kodansha/Springer: Tokyo, 2006; p130.

(9) Krause, A.; Koza, J.; Ispas, A.; Uhlemann, M.; Gebert, A.; Bund, A. *Electrochim. Acta* **2007**, *52*, 6338.

(10) Ueno, S.; Iwasaka, I *J. Appl. Phys.* **1994**, *75*, 7177. Ichioka, S.; Minegishi, M.; Iwasaka, M.; Shibata, M.; Nakatsuka, T.; Ando, J.; Ueno, S *Bioelectromagnetics* **2003**, *24*, 380.

(11) Katsuki, A.; Kaji, K.; Sueda, M.; Tanimoto, Y. *Chem. Lett.* **2007**, *36*, 306. Sueda, M.; Katsuki, A.; Nonomura, M.; Kobayashi, R.; Tanimoto, Y. *J. Phys. Chem. C* **2007**, *111*, 14389.

(12) Fujiwara, M.; Kodoi, D.; Duan, W.; Tanimoto, Y *J. Phys. Chem. B* **2001**, *105*, 3343. Chie, K.; Fujiwara, M.; Fujiwara, Y.; Tanimoto, Y. *J. Phys. Chem. B* **2003**, *107*, 14374. Fujiwara, M.; Chie, K.; Sawai, J.; Shimizu, D.; Tanimoto, Y. *J. Phys. Chem. B* **2004**, *108*, 3531.

(13) (a) Boga, E.; Kádár, S.; Peintler, G.; Nagypál, I. *Nature* **1990**, *347*, 749. (b) He, X.; Kustin, K.; Nagypál, I.; Peintler, G. *Inorg. Chem.* **1994**, *33*, 2077.

(14) Schenck, J. F. *Prog. Biophys. Mol. Biol.* **2005**, *87*, 185.

JP8045565